applied sciences

MDPI

Article

Multi-Year Field Evaluation of Friction, Acoustic Aging, and Permeability Across Diverse Asphalt Pavement Systems

Sung Pil Shin [1], Sang Yum Lee [2,*] and Tri Ho Minh Le [3,*]

[1] Department of Highway & Transportation Research, Korea Institute of Civil Engineering and Building Technology, 283 Goyandae-ro, Ilsanseo-gu, Goyang-si 10233, Republic of Korea; spshin@kict.re.kr
[2] Faculty of Civil Engineering, Induk University, 12 Choansan-ro, Nowon-gu, Seoul 01878, Republic of Korea
[3] Faculty of Civil Engineering, Nguyen Tat Thanh University, 300A Nguyen Tat Thanh Street, District 4, Ho Chi Minh City 70000, Vietnam
* Correspondence: yummy10041004@gmail.com (S.Y.L.); lhmtri@ntt.edu.vn (T.H.M.L.)

Abstract

Urban expressways increasingly struggle with declining skid resistance and rising tire–pavement noise as asphalt surfaces age, yet few studies integrate friction, acoustic behavior, and permeability over multiple pavement types and service years. This research provides the first multi-year, multi-indicator field evaluation of four widely used surface systems in Korea (double-layer drainage asphalt, thin-layer low-noise overlays, SMA, and WC-6) linking wet-skid resistance (BPN), rolling friction (GN), acoustic metrics (LAeq, LAFmax), density evolution, and field permeability (Q) into a single performance framework. A three-year dataset from 2021–2024 (n = 20 sites) revealed that wheelpath friction deteriorated steadily at −1.77 BPN/year, with WC-6 exhibiting the fastest decline (≈−5.5 BPN/year) and drainage asphalt the slowest (≈−2.5 BPN/year). Predicted wheelpath service lives spanned 3.8–5.7 years across pavement types. Acoustic monitoring showed a consistent hierarchy (Drainage < Thin-Layer < SMA < WC-6), with WC-6 producing up to 20 dB higher LAFmax due to strong air-pumping effects. Permeability trends mirrored acoustic behavior, with Q decreasing 9–18% over 3 years but maintaining clear ranking: Drainage > Thin-Layer > SMA > WC-6. SMA NMAS analysis further showed that SMA-10 mm delivers higher initial friction but deteriorates faster than SMA-8 mm. Correlation analysis demonstrated that permeability governs both friction and noise (Q vs. LAeq: r = −0.84; Q vs. GN: r = +0.81), confirming the dominant mechanistic role of void connectivity. Collectively, the findings provide quantitative evidence that drainage and thin-layer systems deliver the most balanced long-term performance across safety, noise, and hydraulic functionality, offering practical guidance for pavement selection on noise-sensitive expressways.

Keywords: asphalt pavement systems; tire-pavement noise; skid resistance; permeability of asphalt; surface aging of asphalt; drainage asphalt; asphalt surface quality

Check for updates

Academic Editor: Syed Waqar Haider

Received: 10 December 2025
Revised: 25 December 2025
Accepted: 26 December 2025
Published: 27 December 2025

Copyright: © 2025 by the authors. Licensee MDPI, Basel, Switzerland. This article is an open access article distributed under the terms and conditions of the Creative Commons Attribution (CC BY) license.

1. Introduction

Skid resistance and tire-pavement noise are two of the most critical surface performance indicators governing roadway safety and environmental quality on urban expressways [1]. As asphalt pavements age, friction progressively declines due to microtexture polishing and binder hardening [2], while acoustic emissions increase as surface voids clog and macrotexture becomes less effective at dissipating tire-induced air pressure [3]. These combined effects elevate crash risk, heighten noise disturbance in densely populated

areas, and accelerate maintenance demands [4]. Despite their importance, most monitoring programs treat friction, noise, and hydraulic functionality as independent parameters, making it difficult for agencies to understand how these mechanisms interact over time or how mixture design choices influence multifunctional long-term performance [5].

Skid resistance deterioration has been widely linked to microtexture polishing, binder aging, and traffic-induced surface wear [6]. Praticò and Briante showed that surface texture evolution is a critical predictor of friction persistence [7]. Studies by Zhang et al. [8] and Hung et al. [9] confirmed that dense-graded pavements lose friction faster due to rapid polishing of fine-textured surfaces, whereas SMA and porous systems maintain more stable microtexture because of stone-on-stone aggregate structure and open void networks.

Tire–pavement noise generation is strongly controlled by air-pumping, tread-block vibration, and surface resonance. Radhika [10] identified tread-impact excitation as a dominant source of high-frequency noise, while Abdukadir et al. [11] demonstrated that vibration transmission increases when surface macrotexture becomes coarse or polished. Studies by Kim et al. [12], Del Pizzo et al. [13], and Yang et al. [14] further showed that low-noise pavements reduce mid-frequency acoustic energy by limiting trapped air and stabilizing tire contact conditions. Acoustic aging investigations by Wrótny and Gardziejczyk [15] consistently confirmed that porous and thin-layer pavements retain quieter performance over time, whereas dense-graded surfaces experience rapid noise escalation.

Porous and drainage pavements have been extensively studied for their multifunctional benefits. Elizondo-Martínez et al. [15] highlighted their hydraulic and environmental advantages, while Mikhailenko et al. [16] and Piao et al. [17] reported improved durability and lower noise when properly designed to delay clogging. Case studies by Lee et al. [18] and Indacoechea-Vega et al. [19] showed that drainage systems consistently outperform dense-graded pavements in acoustic comfort and lifecycle environmental efficiency. Thin-layer low-noise surfacings were also shown by Teti et al. [19] and Zhang et al. [19] to provide mid-level noise reduction without requiring deep porosity.

Permeability plays a critical role in both friction and noise behavior. Park et al. demonstrated that hydraulic flow paths influence water-film thickness, contact stability, and hydroplaning risk [19]. Studies on clogging and hydraulic decay, including Piao et al. [17] and Yang et al. [17], emphasized that drainage pavements maintain higher Q values despite gradual void closure, whereas dense-graded surfaces begin with very low permeability and remain acoustically and hydraulically inefficient over time. Although drainage asphalt is widely recognized for its superior permeability, research shows that clogging rates vary with traffic and environmental exposure, leading to substantial performance divergence across sites. However, quantitative relationships between permeability, friction, and noise remain poorly documented in long-term field studies.

Two major gaps remain in the existing literature. First, few studies integrate friction (BPN, GN), acoustic behavior (LAeq, LAFmax), density evolution, and permeability (Q) into a single multi-year, multi-surface dataset that allows comprehensive cross-mechanistic interpretation. Second, studies seldom compare double-layer drainage surfaces, thin-layer low-noise overlays, Stone Mastic Asphalt (SMA), and dense-graded WC-6, even though these four systems represent the dominant surfacing options on Korean expressways and many international high-speed corridors. Therefore, by quantifying cross-indicator relationships among permeability, friction, and acoustic response, this study advances existing design concepts by demonstrating that permeability can serve as a unifying functional parameter linking safety and noise performance. These findings support the development of performance-based surface selection criteria and integrated pavement management strategies that are transferable to urban expressway networks beyond the Korean context.

To address these gaps, this study conducted a three-year field performance evaluation of four representative pavement systems on an urban expressway network from 2021 to 2024. The research integrates (i) wet-skid resistance (BPN), (ii) rolling friction (GN), (iii) acoustic measurements (LAeq, LAFmax), (iv) compaction index (density), and (v) field permeability (Q) into a unified dataset. Additional SMA testing was performed to assess the influence of NMAS (8 mm vs. 10 mm) on friction behavior. Annual trends, wheelpath effects, deterioration rates, and service-life predictions were evaluated for each pavement type. Finally, a full cross-parameter correlation analysis quantified mechanistic linkages among friction, acoustics, and permeability. This integrated assessment provides agencies and researchers with new multifunctional evidence for selecting optimal low-noise, high-safety pavement systems for modern expressways. Beyond confirming general performance hierarchies, this study provides quantitative field evidence of (a) indicator-specific deterioration rates, (b) threshold-based functional durations for skid resistance and rolling friction, and (c) statistically validated cross-relationships among permeability, friction, and acoustic response derived from a unified multi-year dataset. These results enable direct comparison of surface systems under identical operating conditions and offer actionable insights for performance-based pavement selection and maintenance planning.

2. Materials and Methods

2.1. Overview

Urban expressways in Korea operate under heavy rainfall, high traffic density, and increasing public sensitivity to environmental noise. These conditions intensify hydroplaning risk, reduce nighttime visibility, and elevate wet-weather crash rates, especially in multilane corridors. Tire–pavement noise is also a persistent concern in Seoul, where residential areas are located close to major arterials and noise complaints remain among the most frequent environmental issues.

Low-noise and permeable asphalt technologies, such as SMA, porous/double-layer drainage asphalt, and thin low-noise surfacings, have been widely adopted in countries like Japan and the Netherlands for their proven ability to improve drainage, reduce splash-and-spray, and provide 3–6 dB(A) noise reduction. Although Seoul has implemented several pilot projects, long-term field evidence connecting friction, hydraulic performance, and acoustic aging across different surface types remains limited.

To address this gap, this study conducted multi-year monitoring along major corridors including Gangbyeonbuk-ro, Naebu Ring Road, Olympic-daero, and Dongbu Trunk Road. Functional performance was evaluated using the following:

- Skid resistance (KS F 2375 [20]; BPN and GN)
- Field permeability (KS F 2394 [21])
- Tire–road noise (ISO 11819-2 CPX method [22])

The monitoring program covered 28 sections in total (Table 1), of which 15 primary sections (Figure 1) were used for multi-year friction analysis and 28 sections for CPX noise evaluation, constructed between 2010 and 2024.

Table 1. Summary of pavement types, construction years, properties, and monitoring locations for field sections.

Pavement Type	ID	Year	Thickness	NMAS	Road	Direction	Location/Segment	Length
WC-6 Dense-Graded Asphalt	1	2017	5 cm	13 mm	Olympic-daero	Kangil	120–800 m past Magok Bridge	680 m
	3	~2000	5 cm	13 mm	Gangbyeonbuk-ro	Copper	Seongsu Bridge—Yeongdong Bridge	240 m
	5	2019	5 cm	13 mm	Olympic-daero	Kangil	Cheongdam Bridge—Jamsil Bridge	2.3 km
	8	2020	5 cm	13 mm	Olympic-daero	Kangil	Gwangjin Bridge area	490 m

Table 1. *Cont.*

Pavement Type	ID	Year	Thickness	NMAS	Road	Direction	Location/Segment	Length
	10	2021	5 cm	13 mm	Olympic-daero	Kangil	Seongsu Bridge (−500 m) to (+800 m)	1.3 km
	16	2022	5 cm	13 mm	Olympic-daero	Airport	Gayang Bridge—Magok Bridge	900 m
	19	2023	5 cm	13 mm	Olympic-daero	Airport	Jamsil Bridge—Cheongdam 2 Bridge	1.0 km
	28	2024	5 cm	13 mm	Olympic-daero	Kangil	Yeongdong Bridge—Cheongdam Park	700 m
Stone Mastic Asphalt	2	2017	5 cm	10 mm	Internal circulation	Seongdong	Jeongneungcheon P41–PB1	400 m
	6	2019	4 cm	10 mm	Internal circulation	Seongsan	Hongjecheon P1–P17	760 m
	11	2021	4 cm	10 mm	Gangbyeonbuk-ro	Copper	Seoho Bridge P38–P45	350 m
	13	2015	4 cm	10 mm	Gangbyeonbuk-ro	Copper	Achasan Bridge P22–P32	500 m
	14	2022	4 cm + 4–5 cm	8 mm/10 mm	Internal circulation	Seongsan/Seongdong	Hongjecheon P35–P55	1.0 km
	15	2022	4 cm	10 mm	Internal circulation	Seongsan/Seongdong	Hongjecheon P55–P75 Suseo	1.0 km
	17	2022	5 cm	10 mm	Eastern TL-B	Cheongdam/Jangji	Underpass—Gwangpyeong Bridge	550 m
	21	2023	5 cm	8 mm	Gangbyeonbuk-ro	Nanji	Wonhyo Bridge 465–765 m	300 m
	23	2023	4 cm	8 mm	Internal circulation	Seongsan	P114–P104	478 m
	24	2023	4 cm	8 mm	Internal circulation	Seongdong	P104–P114	478 m
	25	2023	4 cm	10 mm	Internal circulation	Seongdong	P9–P25	780 m
	26	2024	5 cm	10 mm	Olympic-daero	Kangil	Seonsa Apt. resurfaced	400 m
Thin Low-Noise Overlays	4	2017	2 cm	2.5–5 mm	Eastern TL	Offset	Wolleung IC (Sanggye direction)	500 m
	7	2019	2 cm	5 mm	Internal circulation	Seongsan/Seongdong	Bukbu Overpass P33–P38	220 m
	12	2021	1 cm SMP	0–5 mm	Gangbyeonbuk-ro	Copper	Achasan P32–P47	600 m
	27	2024	5 cm	5 mm	Olympic-daero	Kangil	Cheonho Bridge section	300 m
Drainage/Porous Pavements	18	2022	7 cm (double layer)	8 mm/13 mm	Olympic-daero	Gangil/Airport	Gangdong Bridge—+600 m	1.25 km
	20	2023	7 cm	13 mm	Gangbyeonbuk-ro	Copper	Jamsil—Olympic Bridge	384 m
	22	2023	4 cm	10 mm	Gangbyeonbuk-ro	Copper	Mapo Bridge 380–780 m	400 m
	26	2010/2024	5 cm	10 mm	Olympic-daero	Airport/Kangil	Seonsa Apt. section	400 m

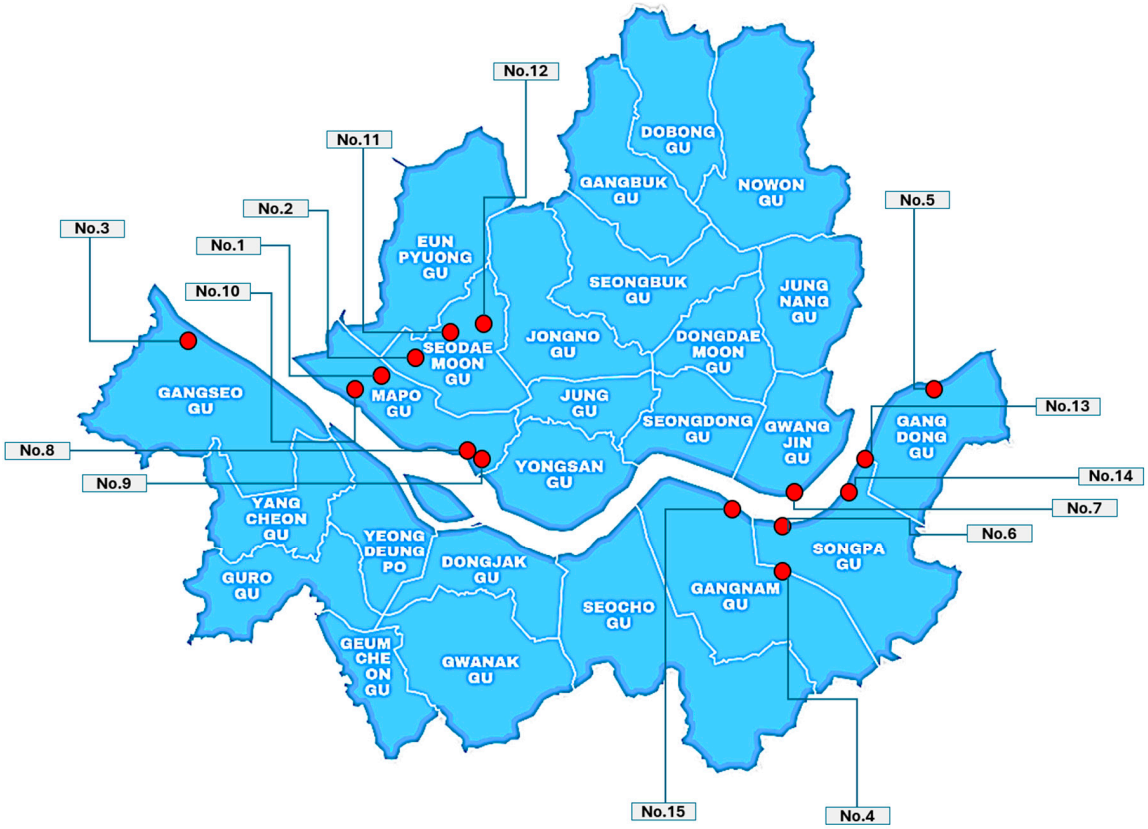

Figure 1. Locations of the 15 main field monitoring sections across the Seoul Metropolitan Road Network.

The following subsections summarize the pavement types used in the monitoring program and describe the field layout and testing procedures adopted for friction, noise, and permeability assessment.

As shown in Table 1, the monitored section lengths vary because the study utilizes existing in-service expressway segments, where pavement type, construction year, and maintenance boundaries are predetermined by the road authority. Each section was selected to ensure uniform surface characteristics (mixture type, age, and traffic condition) and to provide sufficient length for stable friction, noise, and permeability measurements rather than to maintain identical geometric lengths. Therefore, differences in section length do not affect the comparability of the results, as all performance indicators were normalized and evaluated based on consistent measurement protocols.

2.2. Pavement Types Included in the Monitoring Program

The monitoring program covered four representative asphalt surface types widely used on Korean urban expressways: dense-graded rutting-resistant asphalt (WC-6), SMA, low-noise drainage (porous) asphalt, and thin low-noise surfacings. These surfaces differ in aggregate gradation, air-void structure, and surface texture, which in turn control rutting resistance, wet skid resistance, and tire–road noise performance.

This study does not cover all asphalt concrete pavement types used in Seoul; instead, it focuses on four representative surface systems (WC-6 dense-graded asphalt, SMA, thin low-noise overlays, and drainage asphalt) which constitute the dominant surfacing solutions on high-speed urban expressways and noise-sensitive corridors. These pavement types were selected because they capture the full spectrum of surface texture, permeability, and acoustic behavior relevant to expressway safety and environmental performance.

Table 2 and Figure 2 summarize and schematically illustrate the key material, structural, and functional differences among the four pavement systems, highlighting variations in layer configuration, thickness, nominal maximum aggregate size, target air-void structure, and binder modification. The overview of this research is presented in Figure 3.

Table 2. Comparative material and functional characteristics of the four pavement types evaluated in this study.

Pavement Type	Typical Thickness	NMAS	Target Air Voids	Binder/Modification
WC-6 dense-graded	4–5 cm	13 mm	3–5% (low, disconnected)	PG 64–22 or PMA (PG 76–22)
SMA	4–5 cm	8–13 mm	4–6% (mastic-filled)	PMA + cellulose fiber (0.3–0.5%)
Drainage asphalt layer	6–7 cm total	8 mm + 13 mm	10–20% interconnected	PMA (PG 76–22/PG 82–22), RSBS
Thin asphalt layer	2–5 cm	≤5 mm	6–10%, microtexture voids	PMA or proprietary quiet mix

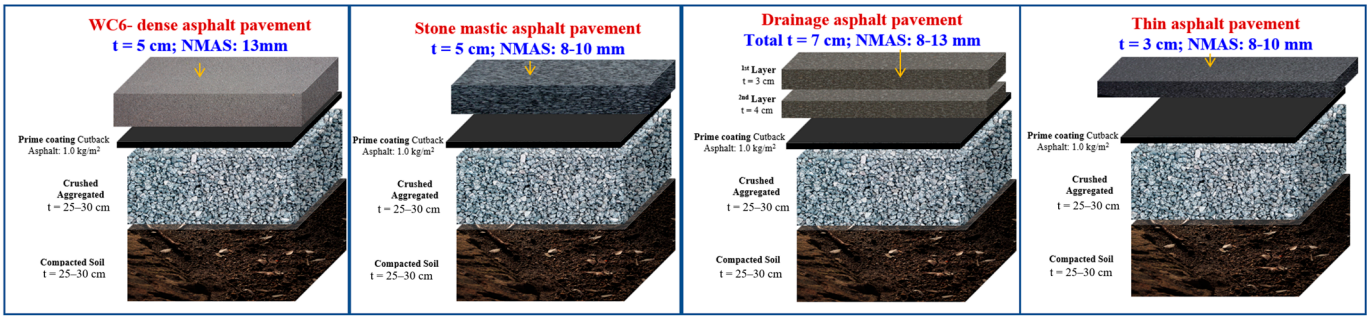

Figure 2. Schematic representation (not to scale) highlighting differences in layer configuration, thickness, and nominal maximum aggregate size among pavement systems.

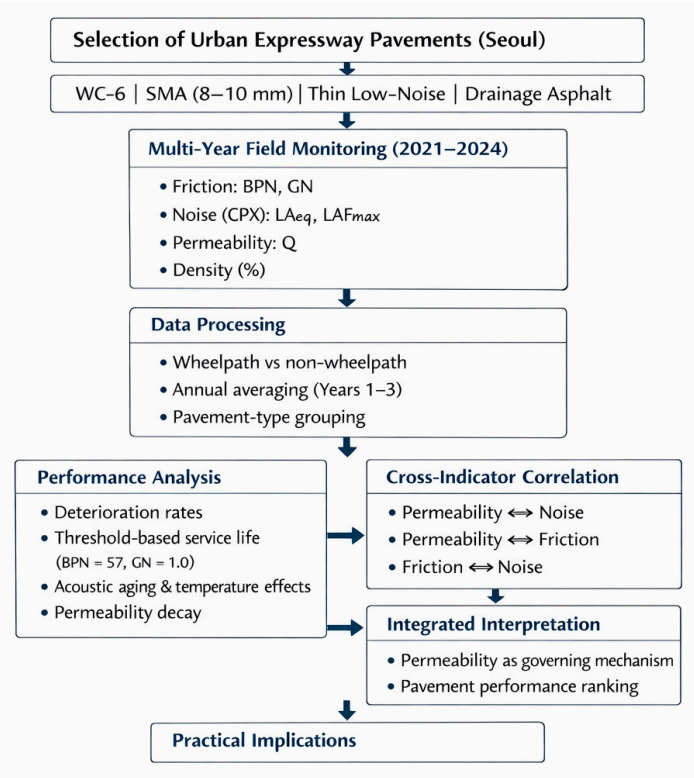

Figure 3. Research flowchart.

2.2.1. Dense-Graded Rutting-Resistant Asphalt (WC-6)

WC-6 is a dense-graded, flow-resistant asphalt concrete commonly applied on heavily trafficked expressways. It typically uses a 13 mm nominal maximum aggregate size and a continuous gradation that produce a tight aggregate skeleton with low air voids, allowing the mix to resist shear deformation under high axle loads and elevated pavement temperatures [11]. Polymer-modified binders are increasingly adopted to enhance rutting resistance and durability under Seoul's summer temperatures (>60 °C) and cold winter conditions (<−15 °C).

Functionally, WC-6 provides reliable structural performance but has limited internal void connectivity and relatively smooth surface texture. As a result, its noise attenuation and wet-weather skid resistance are modest compared with more open-graded low-noise surfaces. In this study, WC-6 sections are used as reference dense asphalt pavements for comparison with SMA, porous drainage, and thin low-noise asphalt.

2.2.2. Stone Mastic Asphalt

Stone mastic asphalt is a gap-graded, stone-on-stone contact mixture comprising a high coarse aggregate fraction, mastic mortar (asphalt binder + filler), and stabilizing fibers (e.g., cellulose) to prevent binder drain-down [23]. SMA surface layers in the monitored network were typically 4–5 cm thick with 8–13 mm nominal maximum aggregate size. The coarse aggregate skeleton carries most of the load, while the mastic fills intergranular voids and improves fatigue and cracking resistance under repeated thermal cycles.

Compared with WC-6, SMA offers enhanced rutting resistance and improved macrotexture, and in many Korean applications exhibits slightly lower tire–road noise. Mixtures with smaller nominal maximum aggregate size (≤10 mm) tend to provide better acoustic performance. However, SMA does not achieve the same noise reduction as porous drainage asphalt and is therefore considered an intermediate low-noise option with good structural durability.

2.2.3. Low-Noise Drainage Asphalt (Drainage Asphalt Layer)

Low-noise drainage asphalt is a porous surfacing technology designed to maintain a high interconnected void content, typically 10–20% air voids, enabling rapid dissipation of rainwater from the tire–road interface [18]. This reduces hydroplaning, splash-and-spray, and nighttime visibility loss. In the present monitoring network, both single-layer porous mixtures and double-layer drainage systems were included; the latter consisted of an 8 mm upper porous layer placed over a 13 mm lower reservoir layer, with a total thickness of about 7 cm. Coarse aggregate contents generally exceeded 80% by mass to maintain void connectivity and structural stability.

Beyond drainage, porous asphalt provides acoustic absorption, particularly at mid–high frequencies. International field studies report typical tire–road noise reductions of 3–5 dB(A) for single-layer porous asphalt and up to 7–8 dB(A) for double-layer systems relative to dense surfaces. Drainage pavements also exhibit superior wet-weather skid resistance because the macrotexture and void network delay water-film formation and maintain friction at higher speeds. However, pore clogging and texture degradation can reduce both hydraulic and acoustic performance over time, highlighting the need for functional monitoring and maintenance.

2.2.4. Thin Low-Noise Surface Treatments (Thin Asphalt Layer)

Thin low-noise surfacings in this study include micro-grinding SMA and proprietary "quiet asphalt" overlays with optimized surface texture and fine aggregate gradation ($\leq$5 mm). These systems are typically 2–5 cm thick and are designed as cost-effective renewal layers [24,25]. Unlike drainage asphalt, thin low-noise surfacings do not rely on large interconnected voids; instead, they reduce noise by controlling surface microtexture, small-scale cavities, and high surface flatness to limit air-pumping and tread-impact mechanisms.

International experience (e.g., Germany, The Netherlands, Denmark, the United States) shows that such thin surfacings can achieve 2–4 dB(A) noise reduction compared with conventional dense asphalt, with improved resistance to void clogging and lower maintenance demands than porous systems. Because they are less sensitive to pore blockage, these mixtures often exhibit better long-term acoustic sustainability. In the context of this study, thin low-noise surfacings represent a next-generation low-noise strategy within Korea's pavement management framework and are evaluated alongside SMA, WC-6, and drainage asphalt for comparative friction and noise performance.

2.3. Testing Methods

2.3.1. Skid Resistance Measurement Methods

Skid resistance was evaluated using two complementary devices: the British Pendulum Tester (BPT) for localized microtexture characterization and a portable Grip Tester for continuous rolling-friction assessment (Figure 4a).



(**a**) (**b**) (**c**)

Figure 4. (**a**) Skid measurement device; (**b**) Noise measurement device; (**c**) Field permeability testing device.

BPT measurements followed KS F 2375 [20] and international procedures. A 1.50 ± 0.03 kg pendulum arm with a 6 × 25 × 76 mm rubber slider was used to generate a 125 mm contact path. Slider wear was checked to remain within allowable limits, and all tests were performed under wet conditions. Pavement-surface temperature was monitored with an infrared thermometer, and the BPN was recorded after reading stabilization.

To capture network-scale friction behavior, a Grip Tester was used to measure dynamic torque-based friction from a rolling test wheel along each pavement section. The resulting GN provides a continuous friction profile that complements the point-based BPN measurements and enables comparison across pavement types and wheelpath conditions.

Korean practice does not specify an asphalt-specific friction threshold; however, the evaluated corridors fall under Category S3 of the Road Safety Facilities Installation and Management Guidelines (MOLIT, 2017 [26]), requiring BPN ≥ 57 (equivalent to SN ≥ 37). This minimum level aligns with intervention criteria used in Japan, the United Kingdom, and EU member countries for high-speed multilane facilities. A summary of the applicable friction requirements is provided in Table 3.

Surfaces with BPN < 57 were classified as entering a friction intervention zone, indicating increased wet-skid risk, particularly during monsoon rainfall.

Skid resistance was evaluated using a self-developed Grip Number tester designed with reference to commercial dynamic friction devices. The system records torque-based friction continuously at 0.2 s intervals along a 14–15 m test path, with the initial and final ~1 m excluded to avoid acceleration artifacts. The measuring wheel, 50 mm in diameter with a 100 mm tread height, provides stable rolling contact, and the resulting Grip Number represents the mean dynamic friction over the central 12–13 m of uniform travel. This approach complements point-based British Pendulum measurements and allows characterization of skid resistance under realistic rolling conditions. Figure 5 presents the Grip Number (GN) profiles measured at two featured test locations, comparing wheelpath and non-wheelpath dynamic skid resistance over the 14–15 m sections, together with corresponding site maps.

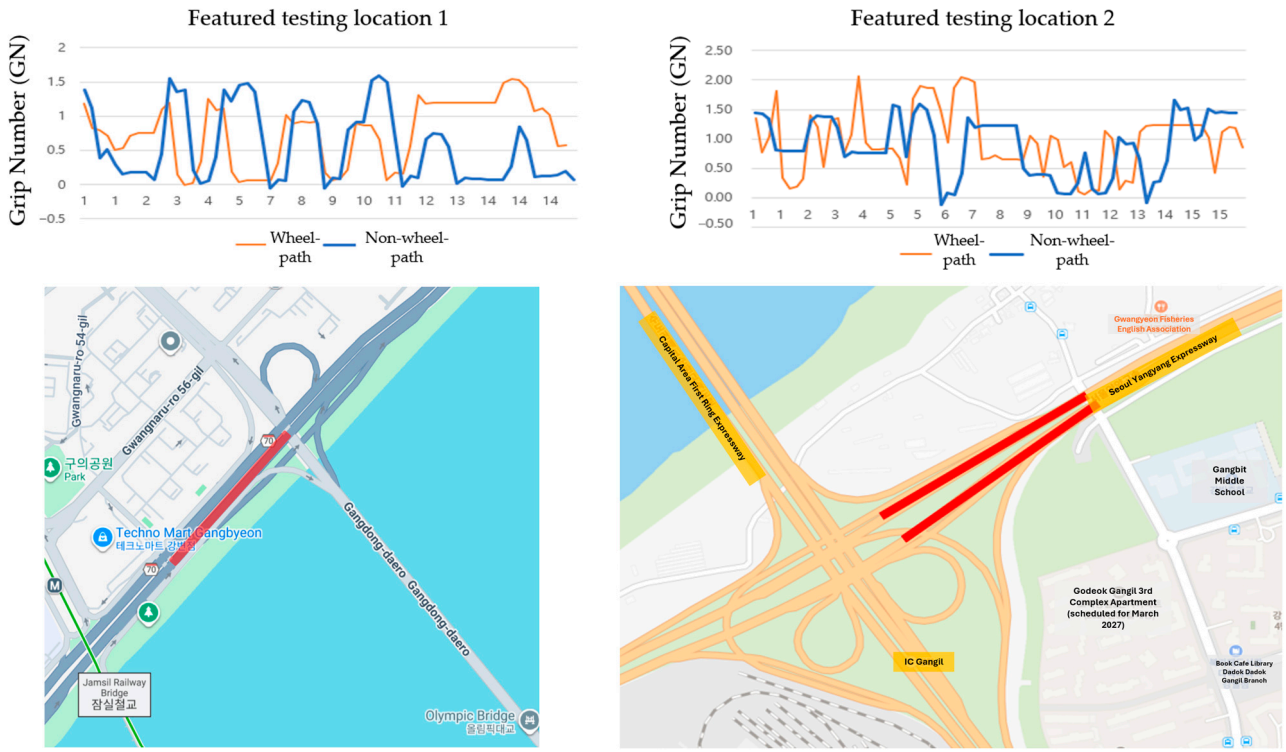

Figure 5. Feature GN testing results.

Table 3. Minimum friction requirements by road category based on Risk Level 3 criteria.

Category	Typical Road Conditions	Minimum Friction (Risk Level 3)
S1	Signal/crosswalk approaches; sharp curves ≥ 5% downgrade	BPN 77/SN 50
S2	Steep grades ≥ 100 m; general highway segments	BPN 67/SN 44
S3 (applied in this study)	Major arterials, expressways	BPN 57/SN 37
S4	Straight low-speed/low-volume sections	BPN 47/SN 31

2.3.2. Close-Proximity (CPX) Tire–Pavement Noise Measurement

Tire–pavement noise was measured using a trailer-mounted CPX acoustic system following ISO 11819-2 [22]. The insulated trailer enclosure reduced interference from wind and background traffic, and dual microphones positioned at ISO-specified locations captured tire–road interaction noise (Figure 4b).

Measurements were conducted at the standard CPX reference speed of 70 km/h. A single reference speed of 70 km/h was adopted in accordance with ISO 11819-2 [22] to ensure consistent comparison across pavement types and service years under controlled operating conditions. Multi-speed CPX testing (e.g., low/average/high speed) can provide additional information on speed sensitivity; however, implementing multiple fixed speeds at each active expressway site was not feasible within the multi-year network monitoring framework due to traffic control constraints and the need to maintain steady-speed measurement windows. Future work should extend the monitoring framework to multi-speed CPX measurements to quantify speed-dependent noise response and improve representativeness under heterogeneous traffic conditions.

Acoustic data were processed in A-weighted 1/3-octave bands from 315 to 5000 Hz, and the overall CPX level (LCpx,P1,70) was computed as the energy-averaged value across the spectrum. For each pavement section, two runs were performed in the same direction, and the final CPX value represents the arithmetic mean of both runs. Noise levels were averaged over 20 m analysis windows to reduce short-range variability caused by texture irregularities and tire vibration.

All CPX noise measurements were conducted using the same trailer-mounted CPX system, reference tire, and test vehicle in accordance with ISO 11819-2 [22]. The vehicle type, tire specification, tire inflation pressure, trailer configuration, and operating speed were kept constant for all pavement sections. As a result, each asphalt surface was subjected to the same input noise conditions, and the measured differences in LAeq and LAFmax reflect variations in pavement surface texture, permeability, and structural response rather than differences in vehicle type or propulsion noise.

2.3.3. Permeability Performance Evaluation Framework

Field permeability was evaluated according to the Seoul Metropolitan Government Low-Noise and Drainage Asphalt Specification (2013) and KS F 2394 [21], which define performance requirements for permeable and drainage asphalt on urban expressways. Functional performance is expressed as the volume of water infiltrating the pavement within a specific time interval. For automobile-only expressways, the required performance level is $Q \geq 1000$ mL/15 s, which was adopted as the evaluation threshold in this study.

To ensure long-term drainage capability, associated mixture criteria include laboratory falling-head permeability (KS F 2494) ≥ 0.01 cm/s. These mixture and field requirements collectively represent the hydraulic and functional durability needed for low-noise and drainage pavements.

Field permeability testing followed the KS F 2394 falling-head method using a standpipe-based permeameter (Figure 4c). The apparatus comprised a 600 mL graduated standpipe, metallic sealing base, porous filter plate, and a weighted U-shaped sealing ring

to ensure watertight contact. The minimum test diameter was maintained at least 10 times the NMAS. Before testing, the surface was cleaned and sealed with oil-based clay.

For each location, the standpipe was filled to the initial head, and the time required for a 400 mL drop was measured. Three repetitions were conducted at approximately one-minute intervals. The permeability index Q (mL/15 s) was calculated as: $Q = 400/t \times 15$, where t is the average discharge time. Measurements were taken in both wheelpath and non-wheelpath positions to capture trafficking effects.

3. Results and Discussions

3.1. Annual Trends and Wheelpath Effects

Annual BPN measurements showed a steady decline in wet-skid resistance across all monitored sections. Pavements constructed in 2022 exhibited consistent deterioration over 3 years, confirming that friction loss is governed mainly by time in service rather than construction year (Figure 6). When results for pavements opened in 2023 and 2024 were normalized to equivalent service intervals, similar trends appeared, indicating that the underlying mechanisms, traffic polishing, binder thinning, and microtexture loss, affect all surface types similarly.

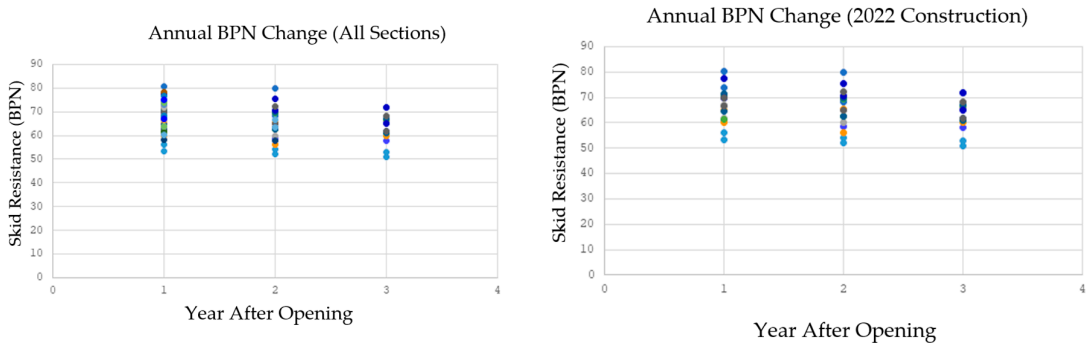

Figure 6. Annual BPN change across the entire network (**left**) and sections constructed in 2022 (**right**). Note: Different colors represent measurement locations/sections used only for visual separation; no categorical or performance significance is associated with color.

When BPN values were aligned by Years 1–3 after opening, wheelpath friction was consistently lower than non-wheelpath friction (Figure 7). Across the network, mean wheelpath BPN was 61.6 compared with 68.1 in non-wheelpaths, yielding a +6.5 BPN difference. Estimated deterioration slopes were −1.77 BPN/year in wheelpaths and −1.64 BPN/year in non-wheelpaths, reflecting the stronger polishing forces and higher shear energy dissipation under direct tire loading. Only sections with at least 2 years of measurements were included to minimize early-age stabilization bias.

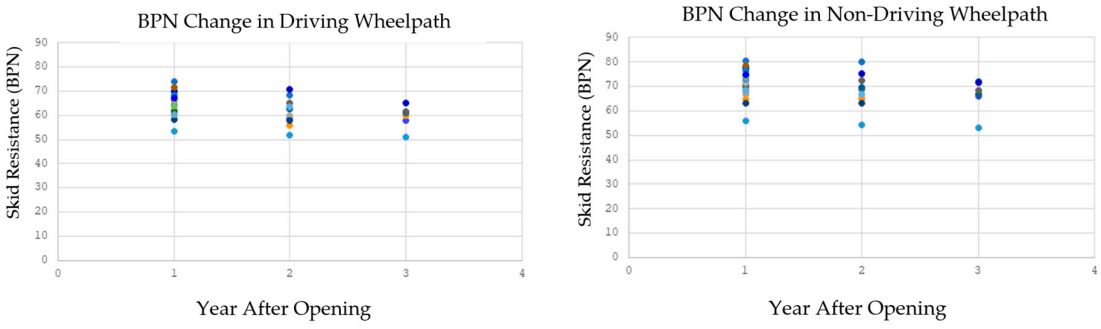

Figure 7. Comparison of BPN change in driving (**left**) and non-driving (**right**) wheelpaths. Note: Different colors represent measurement locations/sections used only for visual separation; no categorical or performance significance is associated with color.

3.2. Pavement-Type Comparisons and Service-Life Interpretation

All sections are located on high-speed urban expressways in Seoul with heavy traffic exposure; however, detailed segment-specific traffic loading histories (e.g., annual AADT, heavy-vehicle fraction, lane distribution) were not available for every site and year in this dataset. To partially address traffic effects, results were reported separately for wheelpath and non-wheelpath locations; nonetheless, traffic-normalized deterioration modeling is identified as a key need for future work.

Figures 8 and 9 show that wheelpath skid resistance declined for all pavement types, but with distinctly different deterioration rates. WC-6 exhibited the fastest reduction (≈−5.5 BPN/year), confirming rapid microtexture polishing typical of dense-graded 13 mm surfaces. Thin layer showed moderate decline (≈−3.5 BPN/year), while drainage asphalt and SMA overlays demonstrated the slowest deterioration (≈−2.5 BPN/year), reflecting their more stable macrotexture and polymer-modified binder systems. Corresponding GN trends produced similar rankings, reinforcing that drainage and thin-layer pavements retain functional friction more effectively under repeated traffic loading.

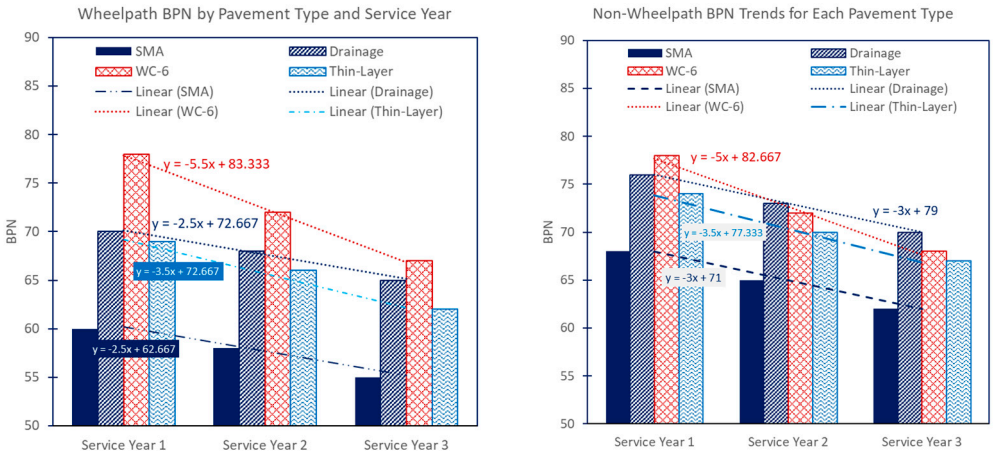

Figure 8. Analysis of wheelpath and non-wheelpath BPN changes by service life.

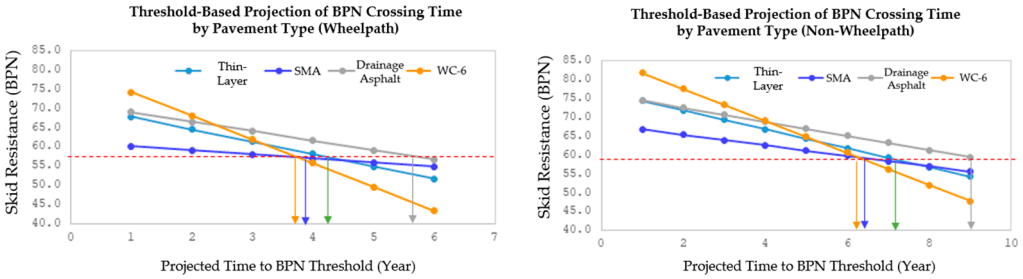

Figure 9. Threshold-based projection of the time required for wheelpath and non-wheelpath BPN values to reach the intervention criterion (BPN = 57), based on linear interpolation of three-year field measurements.

Threshold-based projection using BPN = 57 as the intervention criterion indicated shorter wheelpath durability for WC-6 (≈3.8 years), followed by SMA (≈4.0 years), thin-layer pavements (≈4.4 years), and drainage asphalt (≈5.7 years). Projected threshold-crossing times in non-wheelpath areas were consistently longer, ranging from approximately 6 to 9 years across pavement types. Drainage asphalt exhibited the smallest wheelpath penalty and the longest overall functional duration, whereas WC-6 consistently fell below the network average after the early service period.

These findings are consistent with the observations of Zhang et al. (2020) [8], who similarly reported that dense-graded asphalt experiences the fastest friction deterioration due to rapid microtexture polishing, while porous and SMA surfaces retain higher skid resistance over time because of their more stable macrotexture and interconnected void structure.

Overall, drainage and thin-layer systems provide the most favorable balance between wet-skid durability and functional service life under the same expressway operating conditions.

3.3. Grip Tester Evaluation and Comparison with BPN

GN measurements across 20 sites supported the overall BPN trends, as shown in Figure 10. On average, wheelpath GN was approximately 1.06, compared with 1.19 in non-wheelpaths, indicating 12–13% higher friction potential outside the primary traffic channel. Wheelpath GN represented ~85% of the corresponding non-wheelpath values, slightly lower than the ratio observed for BPN, because GN's 12–13 m continuous footprint captures spatial variability that the point-based BPN does not.

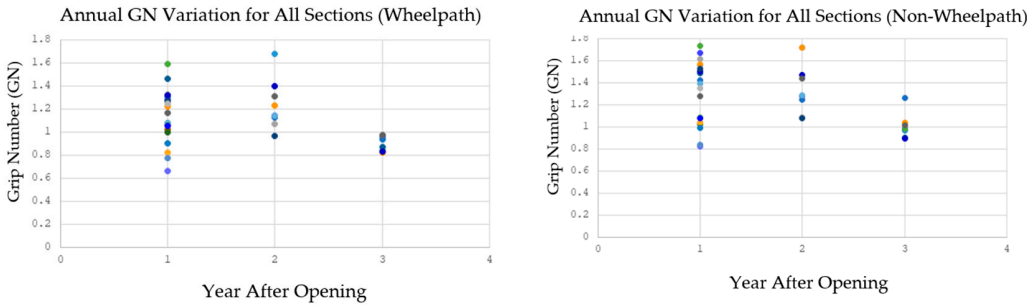

(**a**) (**b**)

Figure 10. Annual GN variation in wheelpath (**a**) and non-wheelpath surfaces (**b**). Note: Different colors represent measurement locations/sections used only for visual separation; no categorical or performance significance is associated with color.

Annual GN data showed gradual decline consistent with cumulative surface polishing. Deterioration rates were −0.117 GN/year in wheelpaths and −0.148 GN/year in non-wheelpaths (Figure 10b). Although non-wheelpath surfaces showed slightly faster nominal GN deterioration, their initial GN was higher and remained above wheelpath values; the trend likely reflects localized moisture pockets and measurement variability rather than true structural degradation.

Figure 11 illustrates the annual evolution of GN for wheelpath and non-wheelpath surfaces across the four pavement types. All mixtures exhibited gradual friction loss over three service years, with wheelpath GN consistently lower due to direct traffic polishing. WC-6 showed the steepest decline (≈−0.10 GN/year), followed by SMA and thin-layer surfaces (≈−0.08 to −0.09 GN/year), while drainage asphalt retained the highest GN and showed the slowest deterioration. These trends confirm the influence of mixture structure, with dense-graded WC-6 being most susceptible to texture wear and open- or thin-layer mixes offering more resilient rolling friction.

Figure 12 illustrates the threshold-based projection of the time required for GN values to reach the intervention criterion (GN = 1.0). In wheelpaths, WC-6 reached the threshold earliest (within approximately 3.0 years), followed by SMA (≈2.8 years), thin-layer overlays (≈2.9 years), and drainage asphalt (≈3.1 years). Projected threshold-crossing times in non-wheelpath areas were consistently longer, extending to approximately 4–7.5 years depending on pavement type. Drainage asphalt again exhibited the smallest difference between wheelpath and non-wheelpath projections, indicating more uniform friction retention across the lane. Overall, the GN-based threshold projections are consistent with

the BPN trends and confirm that drainage and thin-layer pavements provide more stable long-term friction performance compared with WC-6 and SMA.

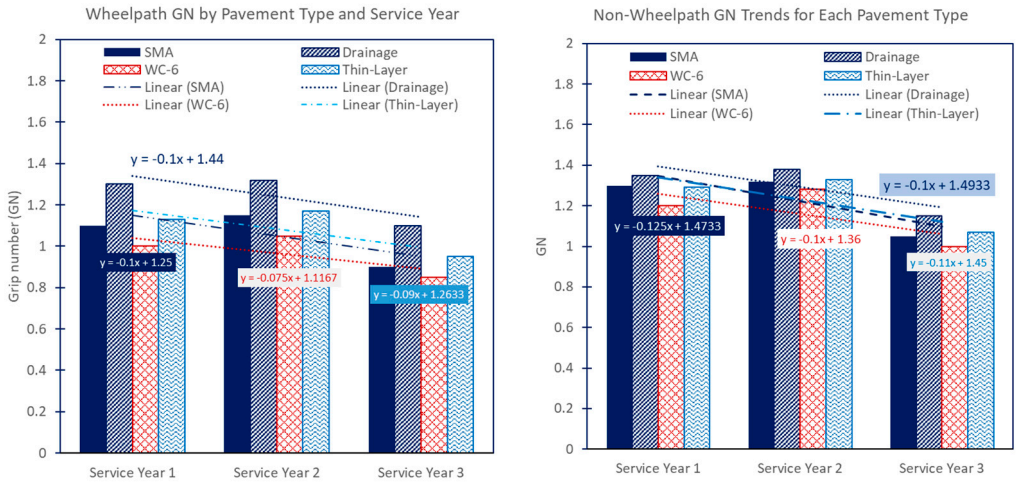

(**a**) (**b**)

Figure 11. Annual GN variation in wheelpath (**a**) and non-wheelpath surfaces; (**b**) changes by service life.

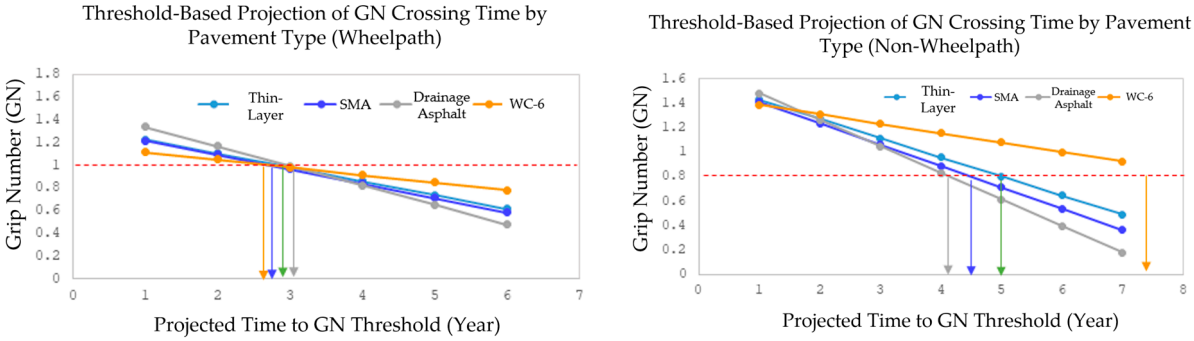

Figure 12. Threshold-based projection of the time required for wheelpath and non-wheelpath GN values to reach the intervention criterion (GN = 1.0), based on linear interpolation of three-year field measurements.

In this research, additional SMA testing was conducted to clarify how variations in NMAS affect both the initial friction characteristics and the long-term deterioration trends of the mixture.

Figures 13 and 14 illustrate the influence of nominal maximum aggregate size (NMAS) on the friction performance of SMA over three service years. In wheelpaths, SMA-10 mm consistently provided higher initial BPN and GN than SMA-8 mm, reflecting the stronger macrotexture and stone-on-stone interlock generated by the coarser aggregate structure. However, SMA-10 mm also exhibited a noticeably faster decline in both BPN and GN between Years 1 and 3, indicating higher susceptibility to microtexture polishing under repeated traffic loading. In contrast, SMA-8 mm began with slightly lower initial friction but maintained a flatter deterioration trend, suggesting more stable long-term texture preservation.

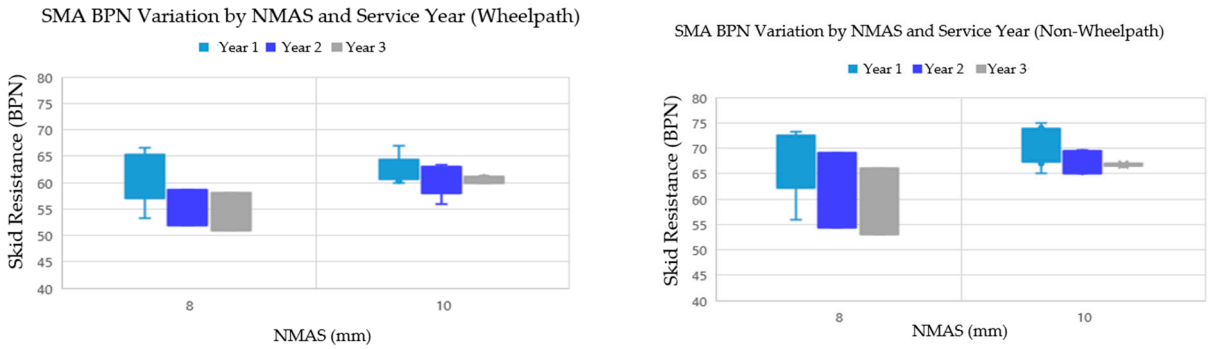

Figure 13. Skid Resistance (BPN) evolution for SMA with 10 mm and 8 mm NMAS.

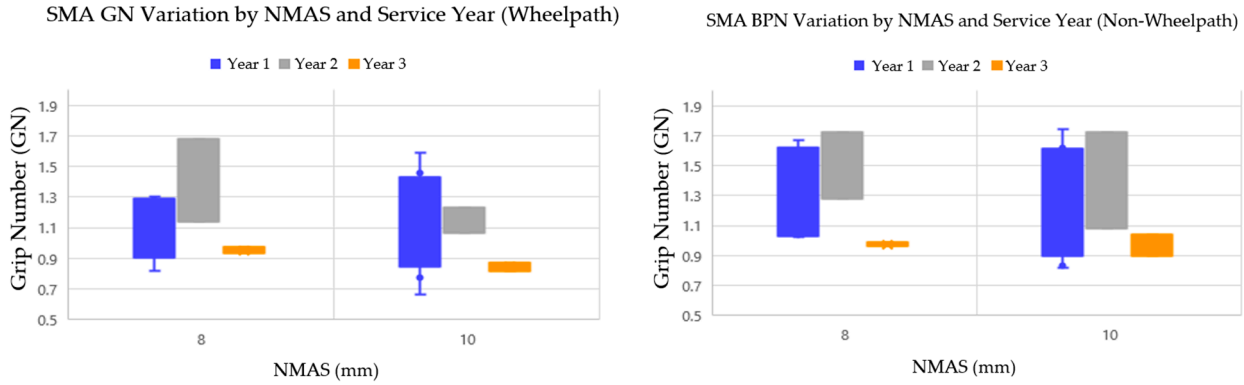

Figure 14. Grip Number evolution for SMA with 10 mm and 8 mm NMAS.

Non-wheelpath results showed the same ranking: SMA-10 mm remained friction-superior in early service but experienced greater texture loss over time, while SMA-8 mm displayed smaller year-to-year variation. GN values followed the same pattern, with SMA-10 mm producing higher Year-1 GN but converging toward or below SMA-8 mm by Year 3. This convergence confirms that coarse NMAS improves early friction but does not guarantee longer functional life.

In this study, the 'service-life' values in Figures 9 and 12 represent a threshold-based projection of the time required for the measured indicator to cross an intervention criterion (BPN = 57; GN = 1.0). Because the monitoring window provides three annual mean observations (Years 1–3), a linear trend was used as a transparent and conservative interpolation within this short period. More complex functional forms (logarithmic, exponential, polynomial) are not statistically robust with three points and may overfit short-term variability; therefore, they were not adopted here. The projections should be interpreted as short-term threshold crossing estimates rather than long-term mechanistic deterioration models.

3.4. Density Trends by Pavement Type (2021–2024)

Figure 15 summarizes the annual mean field density for the four pavement systems—WC-6 dense-graded asphalt, SMA, double-layer drainage asphalt, and thin-layer low-noise overlays—constructed between 2021 and 2024. Overall, all mixtures maintained densities within the expected performance envelope (95–98%), but clear differences emerged between pavement types due to their structural design, void content, and mixture composition.

WC-6 exhibited the highest compaction variability, increasing from 96.6% (2021) to 98.3% (2022) before stabilizing near 98.0% in later years. This reflects its dense aggregate matrix and relatively low air-void content, which makes WC-6 more sensitive to construction rolling temperature and traffic densification during the first year. SMA maintained consis-

tently high densities (97.3–97.6%), supported by its stone-on-stone skeleton and polymer-modified binder system, which resists post-construction densification. Compared to WC-6, SMA densities fluctuated by less than 0.7%, demonstrating superior compaction stability.

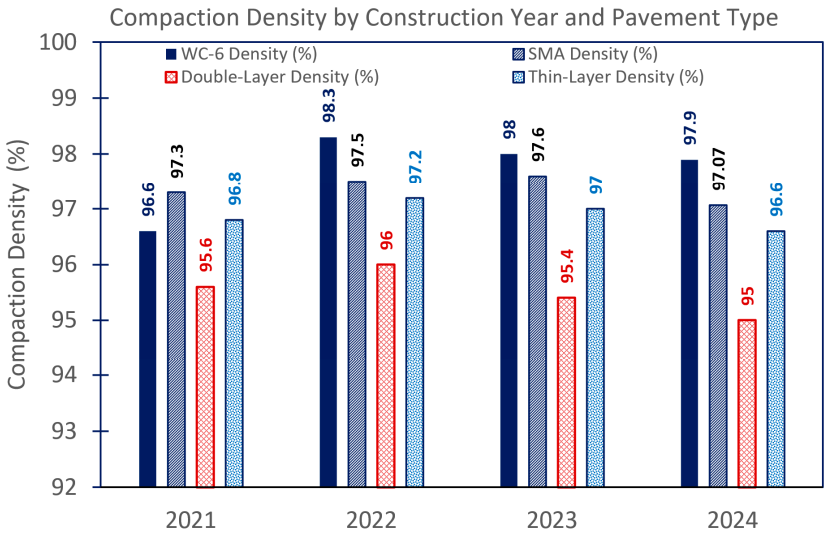

Figure 15. Density (%) by pavement type and year.

In contrast, the double-layer drainage pavement maintained deliberately lower densities (95.0–96.0%) due to its designed macrovoid system. The gradual decline from 95.6% (2021) to 95.0% (2024) corresponds to natural pore-clogging and binder oxidation, which progressively reduce permeability. This trend aligns with the permeability reduction and acoustic aging behavior observed in Section 3.6, where drainage pavements remain quietest despite minor density reductions.

The thin-layer low-noise overlay showed intermediate densities (96.6–97.2%), positioned between SMA and drainage asphalt. Densification during the first service year is moderate due to the thin lift (20–30 mm) and high stiffness of the surface asphalt. The slight decrease from 97.2% (2022) to 96.6% (2024) suggests mild aging and surface compaction but remains within the optimal range to maintain low macrotexture-induced noise.

Comparatively, SMA and thin-layer surfaces show the most stable density profiles (<1% variation), whereas WC-6 exhibits the greatest short-term densification. Double-layer drainage asphalt maintains intentionally lower density levels—approximately 2% lower than SMA and 3% lower than WC-6 on average—consistent with its functional role in permeability and noise reduction. These density differences provide mechanistic support for the acoustic ranking reported earlier (Drainage < Thin-Layer ≈ SMA < WC-6), highlighting the importance of mixture design in controlling noise, permeability, and long-term functional performance.

This overall density pattern is consistent with the general trends reported by several researchers such as Mikhailenko et al. [16], who noted that porous or drainage-type mixtures usually maintain lower densities, while SMA and other stone-on-stone systems tend to show more stable compaction behavior over time

3.5. Acoustic Performance Trends for Drainage, Thin-Layer, SMA, and WC-6 Pavements (LAeq and LAFmax, Years 1–3)

Figure 16a,b present the three-year evolution of average rolling noise (LAeq) and impulse noise (LAFmax) for the four pavement systems. A consistent acoustic hierarchy emerged across all monitoring years, strongly governed by mixture porosity, macrotexture depth, and the continuity of internal void channels. Drainage pavement remained the

quietest surface, with LAeq rising slightly from 61.8 to 62.7 dB(A), a total change of only +1.5%, demonstrating excellent acoustic durability even as partial pore clogging began to develop. Thin-layer low-noise asphalt performed second-best, maintaining LAeq values in the 65–66 dB(A) range, approximately 4–5 dB (6–7%) quieter than SMA and 10–12 dB (15–17%) quieter than WC-6. These differences reflect the thin layer's stiff, smooth surface, which reduces tread-block vibration and limits mid-frequency excitation even with lower permeability than drainage asphalt.

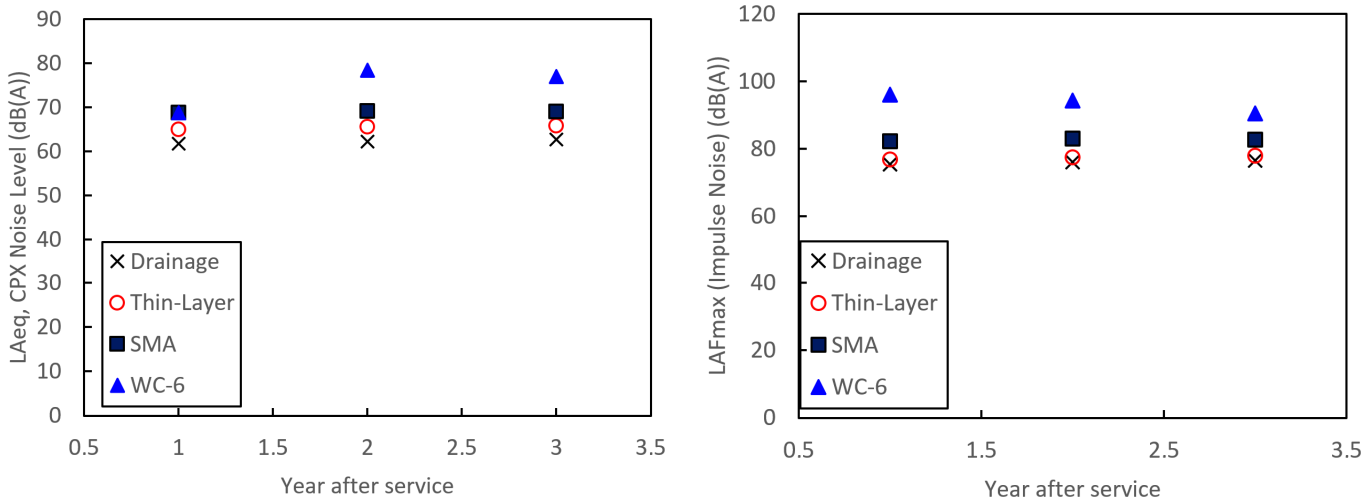

Figure 16. Laeq (**a**) and LAFmax (**b**) noise levels of Drainage, Thin-Layer, SMA, and WC-6 pavements over 3 years of service.

SMA consistently produced higher noise, with LAeq remaining between 68.8 and 69.1 dB(A) and LAFmax increasing only modestly from 82.2 to 82.7 dB(A) (+0.25 dB/year). This stability reflects the persistent coarse macrotexture of stone-on-stone aggregates, which generates increased structural vibration but changes little over time. In contrast, WC-6 dense-graded asphalt exhibited the highest noise levels and the greatest variability. LAeq increased sharply from 68.7 to 78.5 dB(A) between Years 1 and 2 (+14%), before settling at 77.0 dB(A) in Year 3. LAFmax peaked at 96.1 dB(A)—approximately 20 dB (≈26%) louder than drainage pavement—due to strong air-pumping forces generated by its impermeable surface and closed-texture matrix. These large fluctuations indicate that WC-6 is acoustically unstable and highly sensitive to binder hardening, temperature, and traffic polishing.

Overall, the acoustic ranking remained unchanged across the study period, Drainage < Thin-Layer < SMA < WC-6, demonstrating strong mechanistic consistency between mixture design and observed field noise. Drainage asphalt benefits from continuous void pathways that absorb and dissipate pressure waves; thin-layer overlays reduce tread excitation through stiffness and reduced macrotexture; SMA retains coarse texture that intensifies tire–aggregate contact; and WC-6 amplifies both air-pumping and high-frequency vibration due to its dense matrix. This overall acoustic pattern aligns with the broad observations reported by several researchers, such as Del Pizzo et al. [13].

3.6. Temperature-Induced Noise Sensitivity: Morning–Afternoon Differences (ΔLAeq and ΔLAFmax)

Figure 17a,b show the difference between morning and afternoon noise measurements for the four pavement types over three service years. Across all years, drainage pavement

exhibited the smallest sensitivity to temperature, with ΔLAeq values of 0.4–0.5 dB and ΔLAFmax values of 0.8–0.9 dB, indicating stable acoustic behavior even under warmer afternoon conditions. Thin-layer overlays showed slightly higher responses, with ΔLAeq of 0.6–0.8 dB and ΔLAFmax of 0.9–1.1 dB, reflecting minor increases in tread-block vibration as the thin surface softens with temperature.

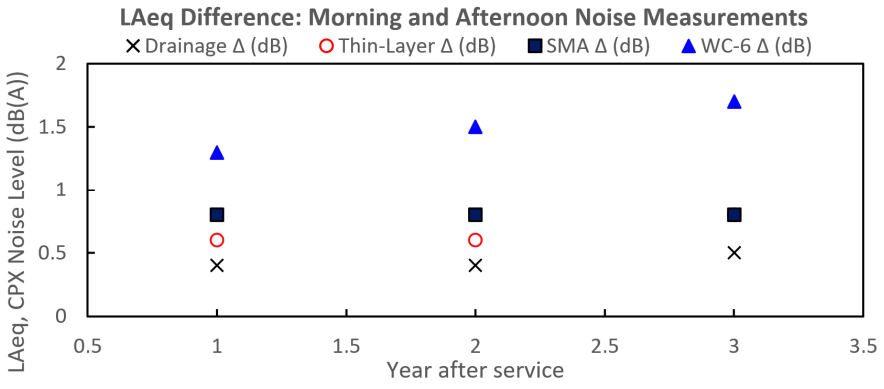

(**a**)

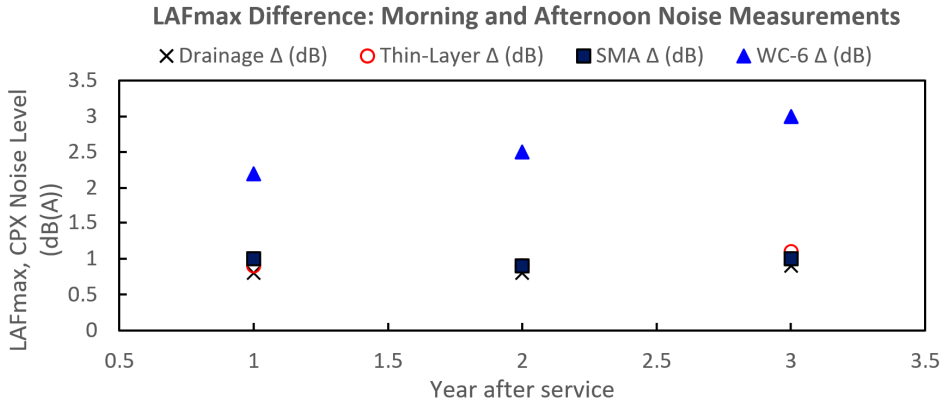

(**b**)

Figure 17. Laeq (**a**) and LAFmax (**b**) difference: morning and afternoon noise measurements.

SMA displayed moderate sensitivity, with ΔLAeq stabilizing at 0.8 dB across all years and ΔLAFmax remaining near 1.0 dB. This consistent behavior is attributable to SMA's stone-on-stone structure, which maintains coarse texture regardless of temperature changes. In contrast, WC-6 dense-graded asphalt showed the highest afternoon noise amplification. ΔLAeq increased from 1.3 dB in Year 1 to 1.7 dB in Year 3, while ΔLAFmax rose dramatically from 2.2 dB to 3.0 dB, representing a 200–300% greater temperature effect than that of the drainage or thin-layer pavements. This strong sensitivity results from WC-6's impermeable surface, which traps air and intensifies air-pumping noise as the binder softens in the afternoon.

Collectively, the results establish a consistent ranking of temperature-driven acoustic sensitivity: Drainage < Thin-Layer < SMA < WC-6. This hierarchy confirms that pavement structure and permeability strongly govern how noise levels respond to daily temperature fluctuations, with porous and thin-layer systems offering superior acoustic stability.

The integrated acoustic indicators in Table 4 further reinforce the long-term performance hierarchy observed across the field monitoring program. Drainage pavement showed the best durability, with modest aging rates for both LAeq (+0.45 dB/year) and LAFmax (+0.60 dB/year), maintaining its position as the quietest system throughout

all 3 years. Thin-layer overlays also demonstrated stable behavior, aging only +0.40 to +0.55 dB/year and consistently ranking second. As shown in Table 4, SMA exhibited minimal acoustic deterioration (+0.05 to +0.25 dB/year), but its inherently coarse macrotexture kept overall noise higher than with porous or thin-layer systems. WC-6 showed the poorest performance, with highly variable aging rates and persistently loud LAFmax peaks linked to strong air-pumping mechanisms. The Acoustic Performance Index (API) highlights these contrasts clearly, Drainage = 1.00, Thin-Layer = 1.12, SMA = 1.35, and WC-6 = 1.72, confirming the superior long-term acoustic efficiency of porous and thin low-noise pavements compared with dense-graded asphalt.

Table 4. Acoustic aging and performance index by pavement type.

Pavement Type	LAeq Aging Rate (dB/year)	LAFmax Aging Rate (dB/year)	Ranking Stability (Years 1–3)	API Score (1 = Best)	Overall Noise Performance
Drainage (Double-layer)	+0.45	+0.60	Always 1st (Quietest)	1.00	Excellent (Quietest and Stable)
Thin-Layer Low-Noise Overlay	+0.40	+0.55	Always 2nd	1.12	Good (Consistent and Quiet)
SMA (8–10 mm)	+0.05	+0.25	Always 3rd	1.35	Medium (Coarse-Texture Noise)
WC-6 Dense-graded	Highly variable	Highly variable	Always 4th (Loudest)	1.72	Poor (Air-Pumping Noise, High LAFmax)

3.7. Featured Case Study: Comparative Acoustic Performance of Drainage, Thin-Layer, SMA, and WC-6 Pavements

A comprehensive comparison of the four representative surface types (double-layer drainage pavement, thin-layer low-noise overlay, SMA, and WC-6 dense-graded asphalt) revealed a distinctly stratified hierarchy of tire–pavement noise performance, as shown in Figure 18 and Table 5. The combined LAeq and LAFmax datasets (morning and afternoon) consistently positioned drainage pavement as the quietest and most stable system, followed by thin-layer, SMA, and finally WC-6, which exhibited the highest noise sensitivity and strongest temperature-dependent amplification.

Drainage pavement provided the most favorable acoustic environment, recording average LAeq values of 61.8–63.2 dB(A) and LAFmax of 75.2–76.9 dB(A) across the monitoring years and time periods (Figure 18a). The frequency spectra showed a pronounced reduction in the 630–1000 Hz band—representing roughly 10–15% lower acoustic energy than that of WC-6. This performance is attributed to the continuous void network that dissipates air-pumping pressure waves and attenuates both impact and high-frequency tread excitation. The morning-to-afternoon noise increase was minimal (+0.4–0.5 dB), confirming the thermal stability of the porous system. Overall, drainage pavement demonstrated superior acoustic comfort, lowest aging rate, and highest-ranking stability.

Thin-layer surfaces delivered intermediate-grade acoustic benefits, with LAeq ranging from 65.0–66.6 dB(A) and LAFmax from 76.5–78.4 dB(A). Although not as quiet as the drainage system, thin-layer consistently remained 2.5–4 dB quieter than SMA and 3–11 dB quieter than WC-6, depending on frequency (Figure 18b). The stiffer, smoother overlay reduced tread-block vibration and limited mid-frequency amplification. Afternoon noise increases remained moderate (+0.6 to +0.8 dB), indicating controlled thermal sensitivity. Thin-layer pavements therefore represent a practical low-noise option when deep porosity or specialized drainage layers are not feasible.

SMA exhibited higher noise signatures, with LAeq values of 68.8–69.8 dB(A) and LAFmax of 81.8–83.3 dB(A) (Figure 18c). The frequency spectra showed a broad mid-frequency hump (500–1600 Hz), consistent with the stone-on-stone skeleton that transfers vehicle-induced vibration more directly to the tire. Acoustic aging was remarkably slow

(+0.05 dB/year), reflecting the durability of coarse aggregate microtexture, but SMA consistently ranked as the third-best performer. Afternoon increases were moderate (+0.8 dB), demonstrating predictable thermal response. SMA remains a structurally durable but acoustically moderate surface type.

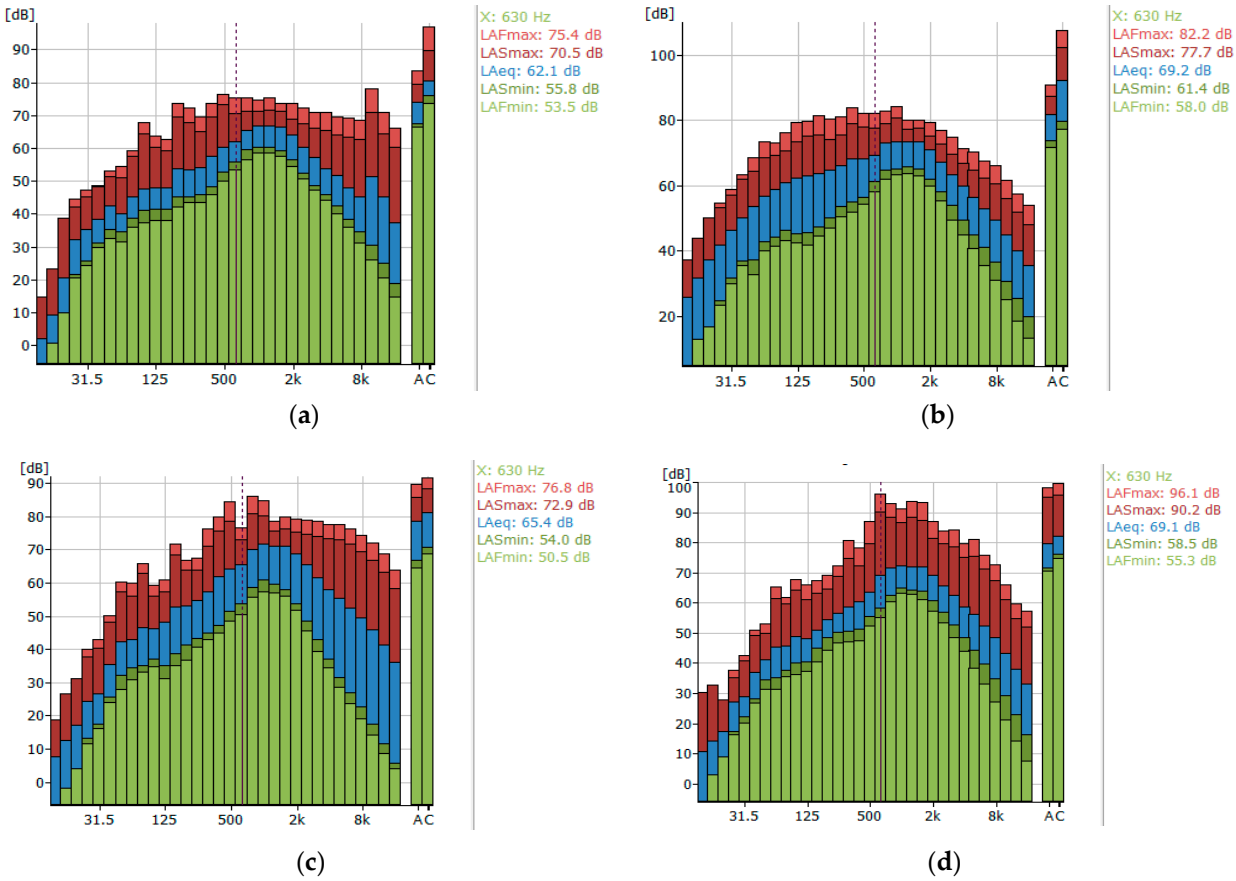

Figure 18. Comparative acoustic performance of Drainage (**a**), Thin-Layer (**b**), SMA (**c**), and WC-6 (**d**) pavements.

Table 5. Frequency-domain noise comparison by pavement type.

Pavement Type	Figure ID	LAeq (dB)	LAFmax (dB)	Dominant Peak (Hz)	Noise Ranking	Primary Mechanism
Double-Layer Drainage Pavement	Figure 18a	62.1	75.4	630–800	Quietest	High void continuity reduces air-pumping and mid-frequency radiation
Thin-Layer Low-Noise Overlay	Figure 18b	65.4	76.8	630–1000	Low–Medium	Thin stiff layer reduces tread excitation
SMA (8–10 mm NMAS)	Figure 18c	69.2	82.2	500–1250	Medium–High	Strong macrotexture + aggregate contact vibration
Dense-Graded Asphalt (WC-6)	Figure 18d	69.1	96.1	630–1600	Loudest	Impermeable surface induces strong air-pumping + high-frequency vibration

WC-6 was consistently the loudest and most acoustically unstable pavement. LAeq values ranged from 68.7–80.0 dB(A), while LAFmax peaked at 95–97 dB(A), over 20 dB higher than that with the drainage pavement (Figure 18d). Afternoon measurements showed the strongest noise surge (+1.3–1.7 dB LAeq; +2.2–3.0 dB LAFmax), caused by intensified air-pumping between the impermeable surface and tire grooves at elevated temperatures. WC-6's smooth, closed texture trapped compressed air and reflected vibration energy, producing the highest CPX noise levels and the most pronounced impulse peaks.

Across all monitoring years and time-of-day conditions, the four pavement systems demonstrated a clear, statistically stable, and mechanistically explainable ranking: Drainage < Thin-Layer < SMA < WC-6. This ranking remained unchanged for all LAeq, LAFmax, frequency-domain, and Δ(morning–afternoon) analyses, affirming the dominant roles of macrotexture depth, connected void structure, surface stiffness, and temperature sensitivity in long-term tire–pavement noise generation. Drainage pavement's robust acoustic durability and minimal thermal response position it as the most reliable solution for noise-sensitive urban expressways. Conversely, WC-6's strong air-pumping behavior and high-frequency amplification highlight the limitations of dense-graded surfaces in noise-critical corridors.

The acoustic patterns observed in the present study are broadly consistent with prior work highlighting the strong influence of surface texture on tire–pavement noise behavior. For example, Del Pizzo et al. [13] reported that tire cavity noise is strongly tied to mega-texture at lower frequencies, a mechanism that conceptually aligns with the higher noise responses observed on denser, less textured surfaces such as WC-6.

3.8. Field Permeability Results

Figure 19 summarizes the three-year evolution of field permeability (Q, mL/15 s) for the four pavement systems. A clear hierarchy was observed, governed primarily by designed air-void content, pore connectivity, and susceptibility to clogging. Double-layer drainage asphalt exhibited the highest permeability across all years, decreasing from 1650 → 1510 → 1360 mL/15 s, corresponding to a 17.6% reduction over 3 years. Despite this decline, drainage pavement remained well above the expressway requirement of 1000 mL/15 s, demonstrating robust hydraulic functionality and sustained pore continuity even under early clogging.

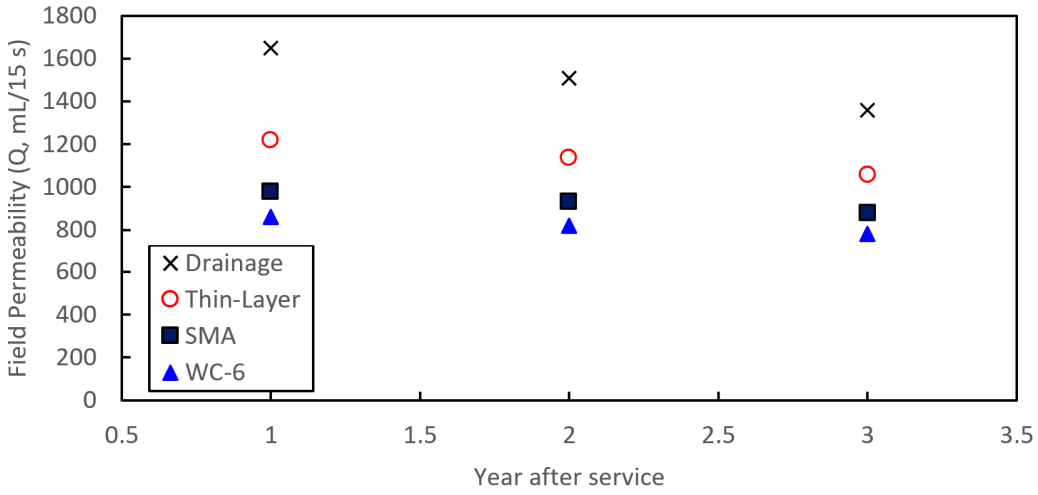

Figure 19. Field permeability (Q, mL/15 s) of Drainage, Thin-Layer, SMA, and WC-6 pavements over 3 years of service.

Thin-layer low-noise overlays showed moderate permeability, reducing from 1220 → 1140 → 1060 mL/15 s (a 13.1% reduction). Although thin-layer pavements are not designed as drainage systems, their partially open texture provides additional flow paths that slowly narrow through binder aging and fine-particle accumulation. SMA displayed lower permeability levels, decreasing from 980 → 930 → 880 mL/15 s (a 10.2% decline), consistent with its stone-on-stone skeleton and lower interconnected void content. SMA remained close to the 1000 mL/15 s threshold, indicating increasingly limited drainage capacity after Year 2.

WC-6 dense-graded asphalt consistently showed the lowest permeability, declining from 860 → 820 → 780 mL/15 s—a 9.3% reduction—and remained well below the typical drainage requirement for high-speed corridors. This low and steadily decreasing permeability demonstrates WC-6's inherently closed matrix, which traps water within the surface layer and accelerates noise-generating air-pumping mechanisms. The relative decline rates confirm that open-graded systems (drainage, thin-layer) experience proportionally greater clogging but maintain higher overall permeability, whereas dense-graded systems begin at low permeability and remain hydraulically restrictive throughout their service life.

Collectively, the permeability ranking remained consistent over 3 years: Drainage > Thin-Layer > SMA > WC-6, mirroring the acoustic performance hierarchy and reinforcing the mechanistic link between void continuity, hydraulic drainage, and noise generation. These results highlight the importance of selecting permeable or semi-permeable surfaces for corridors requiring both noise and safety performance.

These permeability patterns align with the broader understanding in the literature that surface void structure and pore connectivity strongly govern both hydraulic and functional behavior. For example, studies such as Lee et al. [18] reported that porous or semi-porous surfacings maintain superior drainage performance over time due to their continuous void networks, whereas dense surfaces exhibit inherently restricted flow paths.

The consistent agreement between the noise ranking and the permeability ranking supports permeability as a practical field indicator for managing long-term acoustic performance.

3.9. Correlation Analysis Among Friction, Acoustic Response, and Permeability

Figure 20 presents the correlation matrix derived from the combined dataset of BPN, GN, LAeq, LAFmax, and permeability Q across all pavement types and service years. The key novelty of this work lies in translating multi-indicator field measurements into quantified deterioration metrics and cross-functional linkages rather than relying solely on qualitative performance ranking.

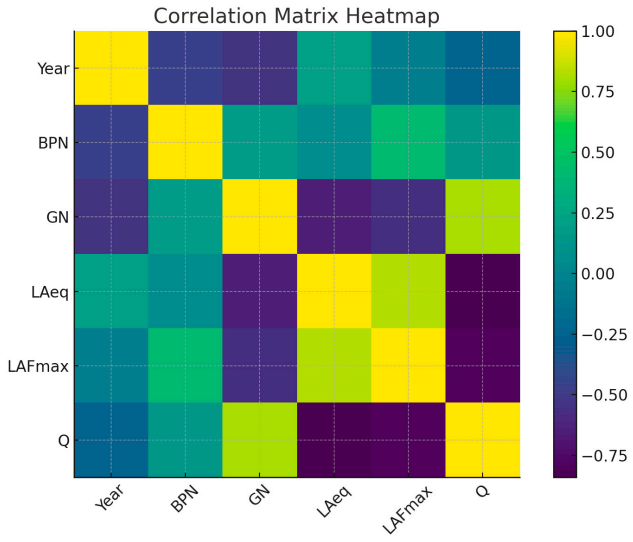

Figure 20. Correlation matrix among friction indicators (BPN, GN), acoustic metrics (LAeq, LAFmax), and permeability (Q).

The correlation analysis was conducted using pooled field observations across pavement types and service years, comprising n = 60 site year observations (20 sites monitored over 3 years). Pearson correlation coefficients are reported together with corresponding significance levels ($p < 0.05$ unless otherwise noted). Because measurements were collected repeatedly at the same sites over time, the analysis is intended to highlight

dominant functional relationships among friction, noise, and permeability rather than to establish fully independent statistical inference. This approach is appropriate for exploratory multi-indicator field assessment and supports mechanistic interpretation of pavement surface behavior.

The results highlight the strong interdependence among functional pavement indicators and reinforce the mechanistic relationships observed in previous sections. GN exhibited the strongest overall associations, showing a strong positive correlation with permeability ($r = +0.81$) and strong negative correlations with both LAeq ($r = -0.64$) and LAFmax ($r = -0.57$). These trends confirm that higher void connectivity not only improves rolling friction but also reduces air-pumping and impact-related noise mechanisms.

Permeability Q demonstrated the most dominant influence on noise behavior, showing very strong negative correlations with LAeq ($r = -0.84$) and LAFmax ($r = -0.79$). This aligns with the superior acoustic performance of drainage asphalt observed earlier and underscores the role of continuous pore pathways in dissipating pressure waves at the tire–pavement interface. Meanwhile, BPN showed weaker correlations with noise indices, indicating that microtexture alone is not the primary determinant of acoustic response. The strong positive relationship between LAeq and LAFmax ($r = +0.83$) further confirms that pavements producing higher steady-state rolling noise also generate more intense impulse peaks.

Collectively, the correlation results validate the multi-parameter interactions underpinning pavement functional performance. High permeability and stable macrotexture support higher friction (GN, BPN) and lower noise (LAeq, LAFmax), whereas dense, low-void surfaces such as WC-6 exhibit the opposite behavior. This integrated evaluation provides quantitative evidence that drainage and thin-layer surfacings offer the most balanced long-term performance across skid resistance, acoustic behavior, and hydraulic function. It should be noted that the dataset includes repeated measurements at the same locations; advanced mixed-effects or time-series models were not applied. Potential autocorrelation effects associated with repeated site measurements may influence absolute correlation strength; however, the consistent ranking and magnitude of correlations across indicators support the robustness of the observed trends. Future studies with longer monitoring periods will enable more rigorous uncertainty quantification.

3.10. Discussions

3.10.1. Integrated Implications for Pavement Performance Modeling and Management

The strong correlations identified in this study, particularly between permeability and both rolling friction and tire pavement noise, extend existing single-indicator evaluation approaches and support the development of integrated performance models. By demonstrating that permeability governs both safety-related and environmental surface functions, the results provide a practical basis for incorporating multifunctional indicators into pavement management systems. Such an approach enables prioritization of surface types and maintenance actions that simultaneously address skid resistance, noise mitigation, and drainage performance, with relevance to metropolitan expressway networks operating under diverse climatic and traffic conditions.

3.10.2. Practical Implications for Tire–Pavement Noise Reduction on Urban Expressways

From a practical perspective, the results suggest several strategies for reducing tire–pavement noise on urban expressways. First, drainage asphalt and thin-layer low-noise surfacings should be prioritized in noise-sensitive corridors, as they demonstrated the lowest LAeq and LAFmax values and the greatest acoustic stability over time. Second, maintaining surface permeability through timely cleaning or preventive maintenance is

critical, since permeability showed the strongest correlation with noise reduction. Third, dense-graded surfaces such as WC-6 should be avoided in locations with high noise sensitivity or large temperature fluctuations, as they exhibited strong air-pumping noise and high afternoon noise amplification. Finally, for stone mastic asphalt, smaller nominal maximum aggregate sizes (e.g., 8 mm) are recommended where acoustic performance is a priority, as they showed more stable long-term noise behavior than coarser SMA mixtures.

Practical takeaway for agencies. Based on the observed hierarchy (Drainage < Thin-Layer < SMA < WC-6) and the quantified deterioration rates, agencies can use permeability (Q) as a screening indicator to jointly manage skid resistance and tire–pavement noise. For noise-sensitive expressways, drainage and thin-layer systems are recommended as primary surfacing options, while dense-graded WC-6 should be limited to corridors where noise is not critical or where additional mitigation measures are feasible. Where porous systems are adopted, periodic permeability-preservation actions (e.g., surface cleaning and clogging control) are expected to provide dual benefits by delaying both friction loss and acoustic aging.

3.10.3. Limitations and Future Research Directions

This study has limitations that should be considered. The three-year monitoring period captures early- to mid-term pavement performance but does not represent full-life behavior, and threshold-based projections were therefore used instead of long-term mechanistic deterioration models.

In addition, detailed traffic loading data were not available for all sections, limiting explicit traffic normalization, and systematic coring or cut-surface imaging was not feasible for all in-service expressway pavements.

As shown in Table 6, the findings from Sections 3.1–3.8 can be interpreted through two complementary lenses: universal behavior governed by fundamental tire–pavement interaction mechanisms, and context-linked behavior influenced by local traffic, climate, and specification frameworks in South Korea. Trends such as wheelpath-controlled friction deterioration, the relative performance ranking of pavement types, the consistency between GN and BPN, and the governing role of permeability are considered universal and are expected to be transferable to other high-speed expressway networks. In contrast, density evolution, absolute permeability levels, and temperature-induced noise amplification are more closely tied to Korean construction practices, climatic conditions, and material specifications, and should therefore be generalized with caution.

Table 6. Classification of key findings from Sections 3.1–3.8 by applicability.

Section	Main Finding	Suggested Applicability
3.1	Progressive friction deterioration with lower wheelpath values	Universal [8]
3.2	Relative friction durability ranking (Drainage > Thin-Layer ≈ SMA > WC-6)	Context-linked (South Korea)
3.3	Consistency between GN and BPN in reflecting surface polishing	Universal [3]
3.4	Density evolution patterns by pavement type	Context-linked (South Korea)
3.5	Stable noise hierarchy among pavement types	Universal [3,8,9]
3.6	Strong temperature sensitivity of dense-graded pavements	Context-linked (South Korea)
3.7	Permeability decay trends and ranking	Context-linked (South Korea)
3.8	Dominant role of permeability in governing noise and rolling friction	Universal [9]

Future studies should extend monitoring duration, incorporate traffic-normalized and non-linear deterioration modeling, include systematic surface imaging, and examine multi-speed noise behavior to further improve international applicability and predictive robustness.

4. Conclusions

This multi-year field investigation provides an integrated assessment of skid resistance, rolling friction, acoustic performance, and permeability across four representative expressway pavement systems in Korea: double-layer drainage asphalt, thin-layer low-noise overlays, SMA, and WC-6 dense-graded asphalt. The combined dataset—spanning BPN, GN, LAeq, LAFmax, density, permeability, and predicted service life—reveals clear and mechanistically consistent performance hierarchies.

(1) Annual friction trends were governed primarily by time in service rather than construction year. Wheelpath surfaces consistently exhibited lower friction than non-wheelpaths, with deterioration slopes of −1.77 BPN/year (wheelpath) and −1.64 BPN/year (non-wheelpath), confirming the dominant effect of traffic polishing and microtexture loss. GN measurements showed a similarly progressive decline and provided a broader spatial representation of surface texture.

(2) Although the role of pavement type in friction performance is qualitatively understood, this study provides quantitative field evidence that friction deterioration rates and intervention-based service life differ markedly among surface systems. Under identical expressway conditions, WC-6 exhibited the fastest BPN deterioration (≈−5.5 BPN/year) and the shortest predicted wheelpath service life (≈3.8 years). SMA and thin-layer pavements showed intermediate performance, while drainage asphalt had the slowest deterioration (≈−2.5 BPN/year) and the longest service life (≈5.7 years). Under identical expressway conditions, WC-6 exhibited the most rapid friction loss and the shortest wheelpath service life, whereas drainage and thin-layer pavements maintained functional friction for up to 1.5–2 years longer, highlighting the practical implications of surface selection for maintenance planning.

(3) Density evolution reflected mixture design and contributed to functional performance differences. WC-6 showed the greatest early densification and variability, while SMA and thin-layer overlays exhibited more stable compaction (<1% variation). Drainage asphalt maintained intentionally lower densities (95–96%), consistent with its designed void network and superior permeability.

(4) A consistent acoustic hierarchy was observed: Drainage < Thin-Layer < SMA < WC-6. Drainage asphalt remained the quietest surface, with minimal acoustic aging and negligible sensitivity to afternoon temperature increases. Thin-layer pavements provided stable low-noise performance, SMA showed moderate mid-frequency excitation, and WC-6 exhibited the highest LAeq and LAFmax values due to pronounced air-pumping mechanisms.

(5) Permeability trends aligned with friction and noise behavior. Drainage asphalt maintained the highest Q values despite early clogging, thin-layer pavements showed moderate permeability decline, SMA approached the drainage limit by Year 3, and WC-6 remained consistently impermeable. These hydraulic characteristics directly mirrored the acoustic and friction rankings.

(6) Correlation analysis quantitatively validated the mechanistic linkages across functional indicators. Permeability Q demonstrated very strong negative correlations with LAeq ($r = -0.84$) and LAFmax ($r = -0.79$), and a strong positive correlation with GN ($r = +0.81$), confirming that void connectivity governs both rolling friction and tire–pavement noise. BPN correlations with noise were weaker, indicating that microtexture alone cannot predict acoustic behavior. The strong LAeq–LAFmax correlation ($r = +0.83$) confirmed synchronized rolling and impulse noise generation on low-permeability surfaces.

Overall, the integrated findings demonstrate that drainage asphalt and thin-layer surfacings provide the most balanced long-term performance across friction, acoustic behavior, density stability, and hydraulic functionality. SMA offers moderate but reliable performance, while WC-6 consistently exhibits the poorest outcomes due to its dense

matrix, susceptibility to rapid polishing, low permeability, and high air-pumping noise. For expressway corridors requiring both safety and noise control, permeable or semi-permeable surface systems are strongly recommended.

Future work should develop unified deterioration models that couple friction, noise, and drainage functions under shared traffic loading and climatic influences. Such models will enable more accurate prediction of long-term performance and inform the refinement of Korea's next-generation specifications for low-noise and drainage asphalt pavements.

Author Contributions: S.P.S. and T.H.M.L.: conceptualization, methodology, writing—original draft. S.Y.L., S.P.S. and T.H.M.L.: visualization, investigation, writing—review, and editing. S.Y.L. and T.H.M.L.: data curation, software. All authors have read and agreed to the published version of the manuscript.

Funding: This study was supported by a research grant from the Ministry of Land Infrastructure and Transport (20250167-006).

Institutional Review Board Statement: Not applicable.

Informed Consent Statement: Not applicable.

Data Availability Statement: Data will be provided on request.

Acknowledgments: We acknowledgment KICT, South Korea, and Nguyen Tat Thanh University, Ho Chi Minh City, Vietnam for supporting this research.

Conflicts of Interest: The authors declare no conflicts of interest, financial or otherwise.

References

1. Zhou, Z.; Zhang, W.; Liang, G.; Chen, B.; Yan, J. Research on the Rolling Process of SMA-13 Asphalt Surface Layer for Bridge Decks Based on Compaction and Skid Resistance Equilibrium Problems. *Buildings* **2023**, *13*, 1510. [CrossRef]
2. Li, W.; Yao, H.; Yang, D.; Peng, C.; Wang, H.; Chen, Z.; Zhao, Y. Study on Pavement Performance of Recycled Asphalt Mixture Modified by Carbon Nanotubes and Waste Engine Oil. *Appl. Sci.* **2023**, *13*, 10287. [CrossRef]
3. Yang, B.; Yuan, M.; Weng, Z.; Li, D.; Leng, Z. Acoustic Aging of Low-Noise Pavements in Hong Kong: Regression Modelling and Mechanism Investigation. *Transp. Res. Part D Transp. Environ.* **2025**, *144*, 104793. [CrossRef]
4. Huang, J.; Yan, K.; Wang, M.; Shi, K.; Li, Y.; Zhang, Y. Performance Evaluation of SBS-Modified Asphalt Mixtures Incorporating Waste Tire Rubber and HDPE. *Constr. Build. Mater.* **2024**, *430*, 136423. [CrossRef]
5. Zhang, H.; Ma, Z.; Huang, Y.; Zhang, Z.; Xiang, X.; Luo, M.; Yu, H. Design and Performance of High-RAP-Content Asphalt Mixture: A Case Study in Jianghe Expressway. *Buildings* **2025**, *15*, 3107. [CrossRef]
6. Wu, Y.; Zhao, Y. Study on Mechanical Characteristics of BRT Asphalt Pavement Structures Based on Temperature Field and Traffic Load. *Appl. Sci.* **2023**, *13*, 3423. [CrossRef]
7. Praticò, F.G.; Briante, P.G. Prediction of Surface Texture for Better Performance of Friction Courses. *Constr. Build. Mater.* **2020**, *230*, 116991. [CrossRef]
8. Zhang, Z.; Luan, B.; Liu, X.; Zhang, M. Effects of Surface Texture on Tire-Pavement Noise and Skid Resistance in Long Freeway Tunnels: From Field Investigation to Technical Practice. *Appl. Acoust.* **2020**, *160*, 107120. [CrossRef]
9. Hung, W.T.; Lam, Y.K.; Mak, K.L. Impacts of Age and Texture of Porous Asphalts on Tyre/Road Noise in Hong Kong. In Proceedings of the NTER-NOISE and NOISE-CON Congress and Conference Proceedings, New York, NY, USA, 19–22 August 2012; Volume 6, pp. 5034–5042.
10. Radhika, B. Study of Dynamic Characteristics of Tread Impact Excitation from Tyre-Pavement Interaction Noise (TPIN) of a Two-Wheeler. *Appl. Acoust.* **2023**, *207*, 109351. [CrossRef]
11. Abdukadir, A.; Yi, J.; Pei, Z.; Chen, Y.; Qiao, Y.; Xiong, Y.; Chu, J.; Feng, D. Study on the Dense-Graded Asphalt Concrete Pavement Correlation between Tire-Pavement Noise and Vibration. *Appl. Acoust.* **2025**, *239*, 110819. [CrossRef]
12. Kim, J.H.; Kim, Y.K.; Alalade, S.; Lee, S.W. Influence of Pavement-Texture Condition on Tire-Pavement Interaction Noise. *KSCE J. Civ. Eng.* **2025**, *29*, 100109. [CrossRef]
13. Del Pizzo, L.G.; Bianco, F.; Moro, A.; Schiaffino, G.; Licitra, G. Relationship between Tyre Cavity Noise and Road Surface Characteristics on Low-Noise Pavements. *Transp. Res. Part D Transp. Environ.* **2021**, *98*, 102971. [CrossRef]
14. Yang, S.; We, Y.; Ye, Z.; Liu, H.; Yang, B.; Liu, W.; Wang, L. Characterization and Modeling of Textured Cement Concrete Pavement Surfaces for Tire-Pavement Noise Prediction. *Appl. Acoust.* **2025**, *227*, 110183. [CrossRef]

15. Wrótny, M.; Bohatkiewicz, J.; Bohatkiewicz-Czaicka, J. Influence of Using Low-Noise Pavements on Residents' Perception of Road Noise Protection. *Transp. Res. Part D Transp. Environ.* **2022**, *113*, 103531. [CrossRef]
16. Mikhailenko, P.; Piao, Z.; Kakar, M.R.; Bueno, M.; Poulikakos, L.D. Durability and Surface Properties of Low-Noise Pavements with Recycled Concrete Aggregates. *J. Clean. Prod.* **2021**, *319*, 128788. [CrossRef]
17. Piao, Z.; Heutschi, K.; Pieren, R.; Mikhailenko, P.; Poulikakos, L.D.; Hellweg, S. Environmental Trade-Offs for Using Low-Noise Pavements: Life Cycle Assessment with Noise Considerations. *Sci. Total Environ.* **2022**, *842*, 156846. [CrossRef]
18. Lee, S.Y.; Man, Y.Y.; Le, T.H.M. Evaluation of Low-Noise-Drainage Pavements with Varied Aggregate Sizes: A Case Study in South Korea. *Case Stud. Constr. Mater.* **2023**, *19*, e02486. [CrossRef]
19. Indacoechea-Vega, I.; Miera-Dominguez, H.; Lastra-González, P.; Castro-Fresno, D. Life Cycle Approach for Evaluating the Environmental and Economic Viability of Low-Noise Asphalt Pavements. *J. Clean. Prod.* **2024**, *466*, 142785. [CrossRef]
20. *KSF 2375*; Standard Test Method for Measuring Surface Frictional Properties Using the British Pendulum Tester. ASTM International West Conshohocken: Conshohocken, PA, USA, 2021.
21. *KS F 2394*; Standard Test Method for Permeability of Porous Pavement. ASTM International West Conshohocken: Conshohocken, PA, USA, 2021.
22. *ISO 11819-2:2017*; Acoustics—Measurement of the Influence of Road Surfaces on Traffic Noise. International Organization for Standardization: Geneva, Switzerland, 2017.
23. Lee, S.Y.; Yun, Y.M.; Minh Le, T.H. Influence of Performance-Graded Binders on Enhancing Asphalt Mixture Performance with Epoxy Resin and Crumb Rubber Powder. *Case Stud. Constr. Mater.* **2023**, *19*, e02628. [CrossRef]
24. Yu, J.; Yang, N.; Chen, F.; Chen, Y.; Lin, Z.; Yu, H. Design of Cold-Mixed High-Toughness Ultra-Thin Asphalt Layer towards Sustainable Pavement Construction. *Buildings* **2021**, *11*, 619. [CrossRef]
25. Saniga, A.M.; Rajish, A.; Shankar, S.; Vishnu, R. Optimal Pavement Maintenance and Management Strategies for Flood Affected Low Volume Rural Roads. *Mater. Today Proc.* **2023**, *in press*. [CrossRef]
26. MOLIT (Ministry of Land, Infrastructure and Transport). *MOLIT Standards System*. Available online: https://www.molit.go.kr/english/USR/BORD0201/m_33276/LST.jsp (accessed on 1 December 2025).

Disclaimer/Publisher's Note: The statements, opinions and data contained in all publications are solely those of the individual author(s) and contributor(s) and not of MDPI and/or the editor(s). MDPI and/or the editor(s) disclaim responsibility for any injury to people or property resulting from any ideas, methods, instructions or products referred to in the content.